Lawrence Berkeley Laboratory
UNIVERSITY OF CALIFORNIA

Physics, Computer Science & Mathematics Division

Submitted to Physical Review Letters

DILEPTON SIGNATURE IN $e^+e^- \to H\ell^+\ell^-$

R.L. Kelly and T. Shimada

October 1980

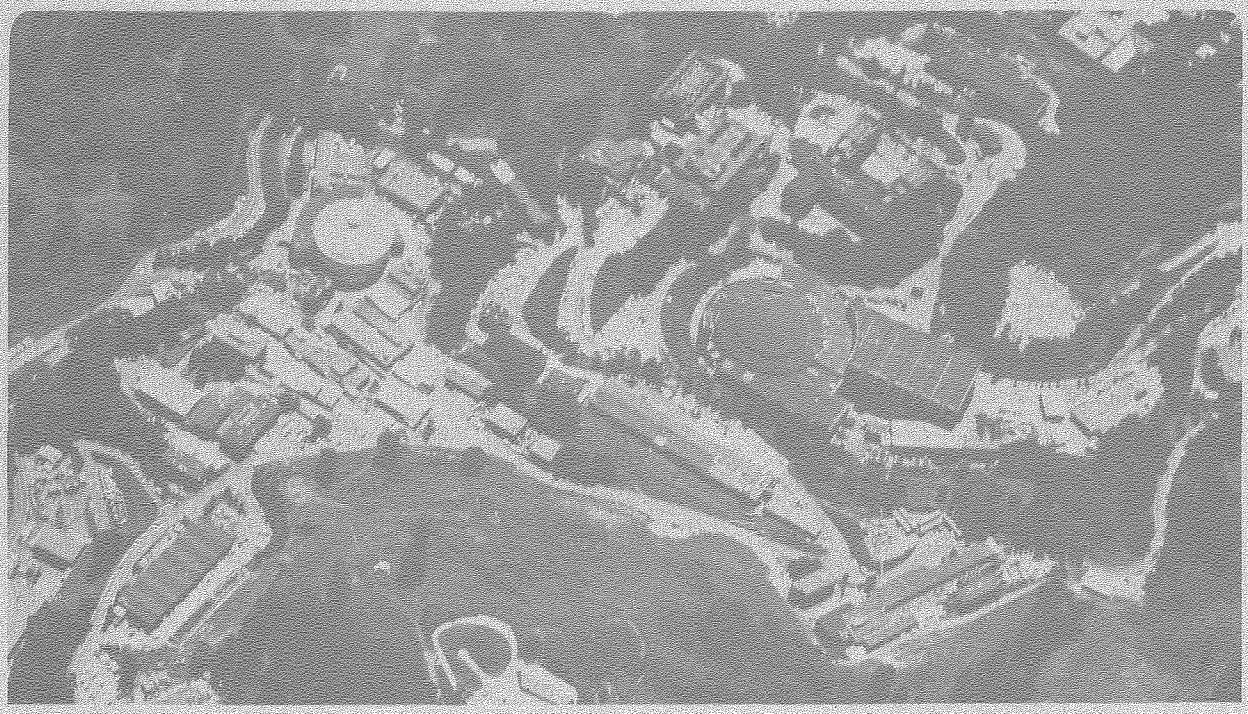

Prepared for the U.S. Department of Energy under Contract W-7405-ENG-48

DISCLAIMER

LBL-11540

October, 1980

Submitted to Physical Review Letters

Dilepton Signature in $e^+e^- \to H\ell^+\ell^-$

R. L. Kelly and T. Shimada

Lawrence Berkeley Laboratory
University of California
Berkeley, CA 94720

Abstract

We calculate the lepton distribution in the reaction $e^+e^- \to$ (Higgs boson) + (dilepton) mediated by a neutral gauge boson. Propagator effects favor a slow dilepton for which the study of the joint angular distribution of ℓ^+ and ℓ^- is an attractive experimental possibility. This distribution is found to be a sensitive probe of the ZZH vertex.

Neutral Higgs bosons are essential ingredients in gauge theories of the weak and electromagnetic interactions with spontaneous symmetry breaking. The possible detection and study of these particles at the next generation of e^+e^- colliding beam machines is of great experimental and theoretical interest.[1,2,3] The direct detection of Higgs particles is expected to be difficult because they couple most strongly to the heaviest available channels which will cascade into complicated multi-particle final states. Much attention has thus been devoted to the indirect detection of the Higgs as a peak in the missing mass spectrum recoiling against the dilepton produced in one of the following reactions mediated by real (Z) and virtual (Z*) neutral gauge bosons:

$$e^+e^- \to Z \to HZ^* \to H\ell^+\ell^- \quad (1)$$

$$e^+e^- \to Z^* \to HZ \to H\ell^+\ell^- \quad (2)$$

$$e^+e^- \to Z^* \to HZ^* \to H\ell^+\ell^- \quad (3)$$

These reactions were first investigated in the Weinberg-Salam[4] (WS) model by Bjorken[5], Ioffe and Khoze[6], and Jones and Petcov[7], respectively. Predicted cross sections are in the picobarn range for $M_H \approx 10$ GeV, and decrease substantially with increasing M_H. A study of rates and backgrounds at LEP[1)] indicates that reaction (1) will be observable up to $M_H \approx 50$ GeV and reaction (2) up to $M_H \approx 100$ GeV. The observation of a peak of the predicted size in the missing mass spectrum of $e^+e^- \to \ell^+\ell^- X$ would be strong evidence for the existence of a Higgs boson. However, alternative interpretations for such a peak exist[8], and even if elementary scalars are produced in this way there may be several Higgs bosons and/or the appropriate gauge group may be larger than $SU(2) \otimes U(1)$ so that the rate turns out to be different from that of the WS model. It will be important to confront further characteristics of such events with theoretical predictions. It addition to energy and mass spectra, which are particularly sensitive to propagator effects, one can consider the angular

distribution of the leptons, which is directly sensitive to the nature of the ZZH vertex. A feature of processes (1) - (3) that is important for the measurement of the leptonic angular distribution is the fact that propagator effects favor a final state Z or Z* that tends to move slowly in the laboratory so that the final lepton momenta are not highly collimated. Calculations of the dilepton mass (M_L) distribution for reaction (1) (Eq. (8) below with $\sqrt{s} = M_Z$) show that the Z* is preferentially produced with a mass close to the endpoint mass, $M_Z - M_H$.[9] For $M_H << M_Z$ the cross section for reaction (2) (Eq. (6) below with $M_L = M_Z$) peaks at[3] $\sqrt{s} \approx M_Z + \sqrt{2}\, M_H$ and for $M_H \approx M_Z$ the cross section peaks at $\sqrt{s} \approx 2.2\, M_Z$. In the kinematic region where reaction (3) is of possible interest, $M_L < M_Z < \sqrt{s}$, propagator effects similar to those encountered in reaction (1) favor dilepton masses close to $\sqrt{s} - M_H$.

Reactions (1) - (3) are all examples of the same basic process, illustrated in Fig. 1, specialized to three different kinematic regions.[10] We assume that the process is mediated by a single neutral gauge boson (generalization to several Z's is not difficult). The relevant interaction Lagrangians are $\mathcal{L}_{ZZH} = 1/2\ g_H Z^\nu Z_\nu H$ and $\mathcal{L}_{\ell\ell Z} = \bar{\psi}\ \gamma^\nu\ (g_V + g_A\ \gamma_5)\ \psi\ Z_\nu$. We will frequently use the coupling constant combinations $C_+ = g_V^2 + g_A^2$ and $C_- = 2\ g_V\ g_A$. In the WS model the coupling constants are $g_H = \kappa\, M_Z$, $g_V = (1/4 - x_W)\kappa$, and $g_A = -1/4\kappa$ where $x_W = \sin^2\theta_W$ and $\kappa = e/\sin\theta_W\cos\theta_W$. We refer to the CM frame angular distribution of the dilepton (equivalently, the decaying Z or Z* in Fig. 1) as the "production" angular distribution, and the distribution of ℓ^+ and ℓ^- in the dilepton rest frame as the "decay" angular distribution.

For unpolarized beams and vanishing lepton masses the predicted production angular distribution, integrated over decay angles, is

$$\frac{d\sigma(e^+e^- \to H\ell^+\ell^-)}{d(\cos\theta)\,d(M_L^2)} = \frac{M_L\ \Gamma_L(M_L)}{\pi\ D(M_L^2)}\ \ \frac{d\sigma(e^+e^- \to HZ^*)}{d(\cos\theta)} \qquad (4)$$

Here θ is the dilepton production angle with respect to the beam axis, $\Gamma_L(M) = C_+ M/12\pi$ is the $\ell^+\ell^-$ width for a Z* of mass M, and $D(M^2) = |M^2 - M_Z^2 + i\Gamma_T M_Z|^2$ where Γ_T is the total width of the Z. Also,

$$\frac{d\sigma(e^+e^- \to HZ^*)}{d(\cos\theta)} = \frac{g_H^2 C_+ Q}{16\pi\sqrt{s}\, D(s)} \left(1 + \frac{Q^2 \sin^2\theta}{2M_L^2}\right) \tag{5}$$

is the differential cross section for $e^+e^- \to HZ^*$ with a Z* of mass M_L and 3-momentum $Q = \lambda^{1/2}(s, M_L^2, M_H^2)/2\sqrt{s}$. A relation equivalent to Eq. (4), but for a $q\bar{q}$ initial state, has been given by Finjord et al.[11] Wherever possible we express our results in terms of M_L and Q so that the qualitative consequences of a slow dilepton, $Q \lesssim M_L$, are apparent. Using Eqs. (4) and (5) we can make contact with previous results on reactions (1) and (2). The integrated form of Eq. (5),

$$\sigma(e^+e^- \to HZ^*) = \frac{g_H^2 C_+ Q(3M_L^2 + Q^2)}{24\pi M_L^2 \sqrt{s}\, D(s)} \tag{6}$$

reduces to the cross section of Ioffe and Khoze[6] for $e^+e^- \to HZ$ when $M_L = M_Z$. The corresponding integration of Eq. (4) gives the cross section for $e^+e^- \to H\ell^+\ell^-$ per unit M_L^2:

$$\frac{d\sigma(e^+e^- \to H\ell^+\ell^-)}{d(M_L^2)} = \frac{12\pi\, \Gamma_L(\sqrt{s})}{D(s)} \cdot \frac{d\Gamma_{H\ell\ell}}{d(M_L^2)} \tag{7}$$

where

$$\frac{d\Gamma_{H\ell\ell}}{d(M_L^2)} = \frac{g_H^2 C_+ Q\,(3M_L^2 + Q^2)}{288\,\pi^3\, s\, D(M_L^2)} \tag{8}$$

is the differential width for the decay of a Z* of mass $\sqrt{s}$ into $H\ell^+\ell^-$. For $\sqrt{s} = M_Z$, Eq. (8) is equivalent to Bjorken's expression[5] for the $H\ell^+\ell^-$ width of an on-shell Z.

The Q^2 factor multiplying $\sin^2\theta$ in Eq. (5) results in a production angular distribution which is rather flat. More pronounced structure is predicted for the decay angular distribution. We have calculated this distribution in the Jackson frame and in the helicity frame.[12] In the Jackson frame the initial e^- momentum lies along the positive z-axis, and in the helicity frame the final Higgs momentum lies along the negative z-axis. The positive y-axis in either frame is defined to lie along the normal to the production plane, $\underline{p}_H \times \underline{p}_{e^-}$. The two frames are thus related by a rotation about the y-axis, but the angle of rotation depends on the CM frame production angle so that the final distributions in the two frames, integrated over production angle, are not simply related. We denote the polar and azimuthal angles of the final state ℓ^- in either dilepton rest frame as θ_F and ϕ_F where F = J or H. The predicted distributions are,

$$\frac{d\sigma}{d\Omega_F d(M_L^2)} = \sum_{LM} \alpha_{LM}^F \, \mathrm{Re}Y_{LM}(\theta_F,\phi_F) \tag{9}$$

where the non-vanishing terms in the sums are,

$$\alpha_{LM}^F(\sqrt{s},\, M_L) = \frac{g_H^2\, Q\, \beta_{LM}^F(\sqrt{s},\, M_L)}{3\cdot 2^8\cdot \pi^{7/2}\, \sqrt{s}\, D(s)\, D(M_L^2)}$$

$$\beta_{00}^J = \beta_{00}^H = 4C_+^2\,(M_L^2 + Q^2/3)$$

$$\beta_{10}^J = 2\sqrt{3}\, C_-^2\, M_L^2$$

$$\beta_{11}^J = -\sqrt{3/2}\,\pi\, C_-^2\, QM_L$$

$$\beta_{20}^J = (2C_+^2/\sqrt{5})\,(M_L^2 - 2Q^2/3)$$

$$\beta_{21}^J = -(\sqrt{3}\,\pi\, C_+^2/\sqrt{10})\, QM_L$$

$$\beta^H_{11} = \sqrt{3/2}\,\pi\, C^2_- M_L\, (M_L^2 + Q^2)^{1/2}$$

$$\beta^H_{20} = -(4C^2_+/3\sqrt{5})\, Q^2$$

$$\beta^H_{22} = (2\sqrt{2}\, C^2_+/\sqrt{15})\, M_L^2$$

The integrated version of Eq. (9) is of more direct experimental interest. This is,

$$\frac{d\sigma}{d\Omega_F} = \int d(M_L^2)\ \ \frac{d\sigma}{d\Omega_F d(M_L^2)} \tag{10}$$

where the integration limits depend on which reaction is being considered. We denote $d\sigma/d\Omega_F$ by an expression similar to Eq. (9) but with α^F_{LM} replaced by σ^F_{LM}. For reaction (1), with a beam energy spread small compared to Γ_T,

$$\sigma^F_{LM} = \int_0^{(M_Z - M_H)^2} d(M_L^2)\ \alpha^F_{LM}\ (M_Z, M_L)$$

For reaction (2) we integrate over M_L^2 in the neighborhood of $M_L \approx M_Z$. Only $D(M_L^2)$ varies appreciably within the resonance width so in this case,

$$\sigma^F_{LM} = \pi\, \Gamma_T\, M_Z\, \alpha^F_{LM}\ (\sqrt{s}, M_Z)$$

For reaction (3) the integration limits are $0 < M_L^2 < (\sqrt{s} - M_H)^2$.

To display the relative size of the various terms in $d\sigma/d\Omega_F$ we define the normalized coefficients $\rho^F_{LM} = \sigma^F_{LM}/\sigma^F_{00}$. In an analogous way we can define an integrated production angular distribution obtained by integrating Eq. (4) in the manner of Eq. (10). This has the form,

$$\frac{d\sigma}{d(\cos\theta)} \propto (1 + \sqrt{4\pi}\, \rho^{CM}_{20}\, Y_{20})$$

where one finds that $\rho^{CM}_{20} = \rho^H_{20}$. For reaction (1) the coefficients ρ^F_{LM} are functions of M_H/M_Z, and for reaction (2) they are functions of Q/M_Z. The L = 2

coefficients are independent of g_H, g_V, and g_A, but the smaller L = 1 coefficients depend sensitively on x_W since they are proportional to $(1/4 - x_W)^2$ times large numerical factors. For reaction (1) there is also a parametric dependence on Γ_T/M_Z, but this is only important for very small Higgs masses, $M_H \lesssim O(\Gamma_T)$. Calculated values of ρ^F_{LM} for reactions (1) and (2) are shown in Figs. 2 and 3. For L = 1 we have used $x_W = 0.23$. For reaction (1) we have used $\Gamma_T/M_Z = 0.03$. In Fig. 3 we give results up to $Q/M_Z = 1$; for $M_H \lesssim O(M_Z)$ the peak rate for reaction (2) is well within this range. At Q = 0 the Jackson frame angular distribution of Eq. (9) is proportional to that for Z-mediated $e^+e^- \to \ell^+\ell^-$, i.e., $C_+^2\ (1 + \cos^2\theta_J) + 2\ C_-^2\ \cos\theta_J$. This accounts for the large values of ρ^J_{20} and ρ^H_{22} seen in Fig. 2 for small M_H, and in Fig. 3 for small Q.

In obtaining $d\sigma/d\Omega_F$ we have integrated over production angles and dilepton masses, in effect assuming uniform lepton acceptance. A realistic calculation for a specific detector would require these integrations to be weighted by the experimental acceptance, and this will lead to (calculable) distortions in the angular distribution. In particular, there are terms proportional to C_+^2 Re Y_{21} and $C_-^2 Y_{10}$ which can contribute to the decay angular distribution in the helicity frame if the acceptance is non-uniform.

All of the above results apply to unpolarized $e^\pm$ beams. It is expected that the SLAC Linear Collider will have a polarized electron beam[13] and there exist various possibilities for polarizing both LEP beams[14]. Longitudinal polarization in either or both beams has the effect of replacing the $C_\pm$ factors from the initial vertex by polarization-dependent coupling constant combinations. This affects the overall magnitude of the production angular distribution and scales all of the coefficients ρ^F_{1M} by a common factor, but leaves the coefficients ρ^F_{2M} unchanged. Simultaneous transverse polarization

in both beams induces an azimuthal dependence in the production angular distribution, but like the $\sin^2\theta$ term it is proportional to Q^2 and is correspondingly suppressed. Transverse polarization has no effect on the decay angular distributions of Eq. (9). The effect drops out due to integration over the azimuthal production angle.

Our interest in this investigation developed from stimulating discussions with Ian Hinchliffe. Our work was supported by the U. S. Department of Energy under Contract No. W-7405-ENG-48. RLK acknowledges the hospitality of the CERN Theory Division where part of this work was done.

References

1. G. Barbiellini et al., The Production and Detection of Higgs Particles at LEP, ECFA/LEP Working Group, SSG/9/4 (1979).
2. M. K. Gaillard, Comments on Nuclear and Particle Physics 8, 31 (1978).
3. J. Ellis, M. K. Gaillard, and D. V. Nanopoulos, Nucl. Phys. B106, 292 (1976).
4. S. Weinberg, Phys. Rev. Letters 19, 1264 (1967).
   A. Salam, Proc. 8th Nobel Symposium, Stockholm (1968), ed. N. Svartholm (Amqvist and Wiksell, Stockholm, 1968), p. 367.
5. J. D. Bjorken, Proc. 1976 SLAC Summer Institute, SLAC-198, 1976, p. 1. A factor of π is missing from the denominator of the right-hand side of Eq. (4.30), but the branching ratio given in Fig. 11 is correct.
6. B. L. Ioffe and V. A. Khoze, Fiz. Elem. Chastits At. Yadra 9, 118 (1978) [Sov. J. Part. Nucl. 9, 50 (1978)].
7. D. R. T. Jones and S. T. Petcov, Phys. Lett. 84B, 440 (1979).
8. M. A. B. Bég, H. D. Politzer, and P. Ramond, Phys. Rev. Letters 43, 1701 (1979). The coupling of a CP = -1 composite scalar to Z's is similar to the coupling of a π^0 to two photons (cf. $\mathcal{L}_{ZZH}$).
9. J. Finjord, Physica Scripta 21, 143 (1980).
10. An exception to this is reaction (3) with e^+e^- in the final state. Our results do not apply to this reaction in the kinematic region where it has important contributions from Z-exchange (see Ref. 7).
11. J. Finjord, G. Girardi, and P. Sorba, Phys. Lett. 89B, 99 (1979).
12. E. Byckling and K. Kajantie, Particle Kinematics, Wiley (London), 1973.
13. SLAC Linear Collider Conceptual Design Report, SLAC-Report-229, 1980.
14. LEP Study Group, CERN/ISR-LEP/79-33, 1979.

Figure Captions

Fig. 1. Feynman diagram for reactions (1) - (3).

Fig. 2. Angular distribution coefficients for reaction (1).

Fig. 3. Angular distribution coefficients for reaction (2).

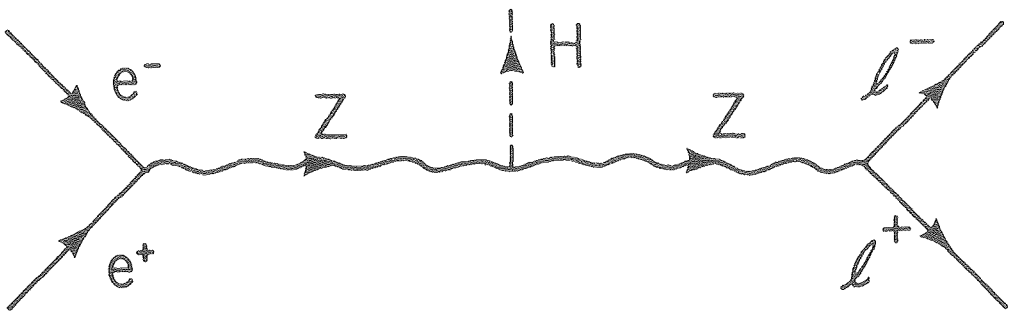

XBL 809-4413

Figure 1

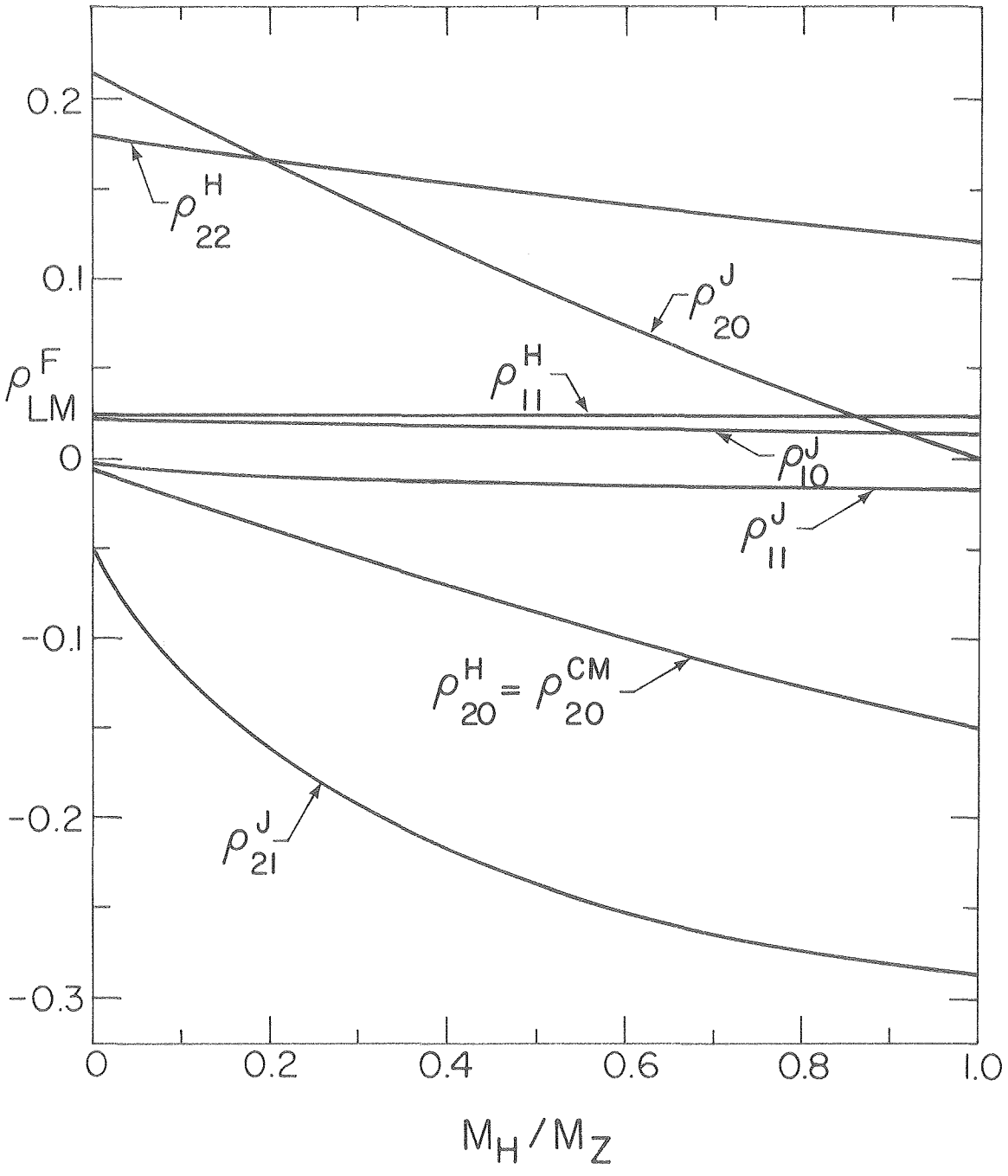

XBL 8010-2172

Figure 2

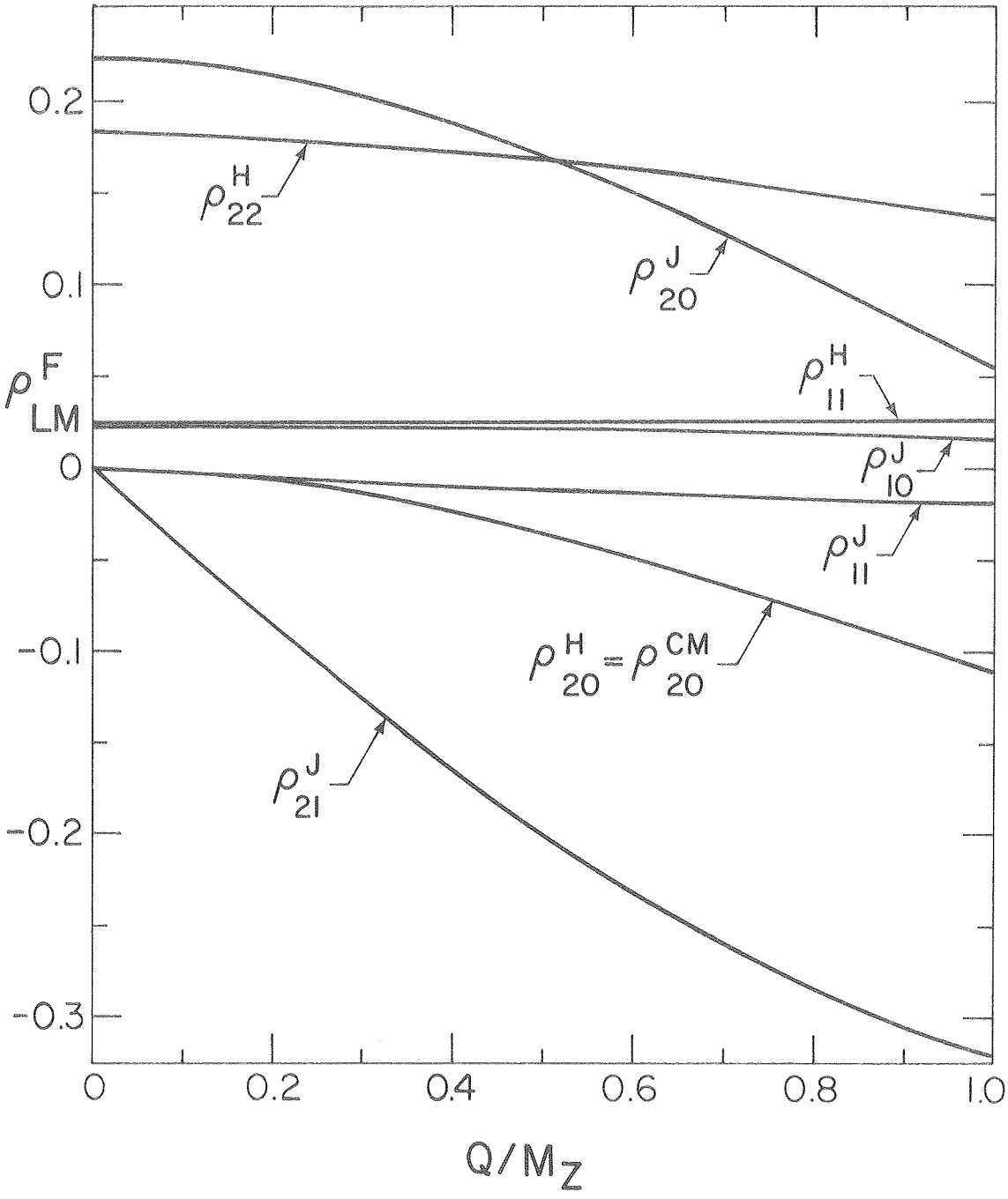

XBL8010-2173

Figure 3